

Structure Refinement of TiCu_7Se_4 from X-Ray Powder Profile Data

LARS ERIKSSON AND PER-ERIK WERNER

*Department of Structural Chemistry, University of Stockholm,
S-106 91 Stockholm, Sweden*

ROLF BERGER

*Institute of Chemistry, University of Uppsala, Box 531,
S-751 21 Uppsala, Sweden*

AND ALAIN MEERSCHAUT

*Laboratory of Solid State Chemistry, UM-CNRS No. 0110 University of
Nantes, Box 1044, F-44037 Nantes, France*

Received June 1, 1990

The structure of TiCu_7Se_4 (synthetic crookesite) has been refined from X-ray powder data using the Rietveld technique. The compound is isostructural with $\text{NH}_4\text{Cu}_7\text{S}_4$ and TiCu_7S_4 , although successful refinements from two independent data sets (both with $R_F = 6.4\%$) occurred in $I4/m$ rather than $\bar{I}4$ previously suggested for this structure type. Positional parameters of natural crookesite were refined from somewhat inferior single-crystal data to $R_F = 8.5\%$. © 1991 Academic Press, Inc.

Introduction

In a recent phase-analytical study of the Ti-Cu-Se system (1) five new ternary phases were synthesized and, subsequently, characterized by powder diffraction and chemically analyzed by microprobe technique on polished single crystals. Further crystallographic characterization has proceeded in the form of refinements based on well-founded structural hypotheses (2) for the structures of TiCu_3Se_2 (3), TiCu_5Se_3 (4), and $\text{Ti}_3\text{Cu}_4\text{Se}_{10}$ (5).

As previously discussed (1, 6), TiCu_7Se_4 must be viewed as synthetic *crookesite*, a mineral that is slightly copper-deficient compared with the above stoichiometry. Weissenberg film results implied body-cen-

tering and Laue symmetry $4/m$, consistent with the space groups $I4/m$, $I4$ or $\bar{I}4$. Since the long-term controversy as to the exact composition of the mineral was now solved, and a similar compound was characterized in the Ti-Cu-S system (7), literature research pointed toward isostructurally with $\text{NH}_4\text{Cu}_7\text{S}_4$ (8). The same conclusion was independently reached by Johan (9) at approximately the same time.

However, the structure of the type compound was determined more than thirty years ago from limited film data using Fourier techniques (8). In the figure presenting a projection of the crystal structure of $\text{NH}_4\text{Cu}_7\text{S}_4$, the z-coordinates of some copper atoms belonging to one of the $8g$ sites in $\bar{I}4$ (with ideally 75% occupancy to account

for correct stoichiometry) are in conflict with the body-centering condition. The question arises whether the dataset was marred, and whether a model with higher symmetry would be permissible. The mistake at least led to wrong conclusions as regards the *distance* between the copper atoms on this 8g site, creating an anomalously short contact of 1.64 Å.

Preliminary intensity calculations on TlCu_7Se_4 (6) and TlCu_7S_4 (7) had shown good agreement with observations also by constraining all z-coordinates to 1/4 (3/4), in fact a situation corresponding with $I4/m$ symmetry. While discussing the TlCu_5Se_3 structure (4) we noted that the formal structural relationship $\text{TlCu}_5\text{Se}_3/\text{TlCu}_7\text{Se}_4$ has a direct counterpart in $\text{RbLiZn}_2\text{O}_3/\text{RbLiZn}_3\text{O}_4$ (21, 22) with space groups $P4_2/mnm$ and $I4/m$, respectively. The former symmetry is in accordance with that found for TlCu_5Se_3 .

In view of all these facts it seemed worthwhile to take a closer look at TlCu_7Se_4 to ascertain whether $I4/m$ were a possible alternative. We had no crystals available of the synthetic compound. On the other hand, it was possible to extract crystalline material for diffractometry from a crookesite sample. However, difficulties arising in the course of that study prompted us to proceed with powder diffractometry on the synthetic product instead. This paper summarizes the results of the single-crystal and powder profile refinements, showing that TlCu_7Se_4 is reasonably well described by using $I4/m$ rather than $I\bar{4}$.

Sample Preparation and Characteristics

Powder material. The preparation of synthetic crookesite occurred at 670 K, as previously reported (1). According to powder diffraction the sample contained a trace of a second phase, identified as Cu_2Se in a low-symmetry modification (10). The presence

of this phase did not interfere with the structure solution.

Crystal material. In a solid sample of crookesite, recently taken from the Skrikërum mine, Sweden, some parts could be discerned that looked better crystallized than the remaining more fine-grained material. Although brittle, the crystals showed poorly developed cleavages and a morphology not easy to describe. The same problem was mentioned by Earley (11) in his X-ray investigation of the mineral. The crystal selected for single-crystal diffractometry was approximately a parallel epiped with dimensions (mm) $0.2 \times 0.1 \times 0.08$.

Single-Crystal Diffraction

For the crystals a CAD4 (Enraf-Nonius) diffractometer equipped with graphite monochromatized $\text{MoK}\alpha_1$ radiation was used. Reflexions were recorded using an ω -scan ($\Delta\omega = 1.5 + 0.35 \tan \Theta$) in half of reciprocal space ($\pm h, \pm k, l$). However, averaging of the intensities belonging to equivalent reflexions did not yield a satisfactory result. The lowest R -value of a refinement was obtained for a dataset with h, k, l all positive. In the range $0 < \sin \Theta/\lambda \leq 0.75$ ($1.5 \leq \Theta \leq 32$) 153 reflexions were measured with $I \geq 2.5 \sigma_I$. Two reflexions, (321) and (004), had to be discarded owing to extensive secondary extinction, which could not be corrected for with the extinction factor refined to $g = 6.66 \cdot 10^{-7}$. The weighting scheme used in the refinement (24 parameters) was $w^{-1}(F_0^2) = \sigma^2(I) + (0.07 F_0^2)^2$.

Powder Diffraction

X-ray powder diffraction photographs were taken with a Guinier-Hägg type subtraction-geometry focusing camera equipped with $\text{CuK}\alpha_1$ radiation ($\lambda = 1.5405981$ Å). Single-coated film (CEA Reflex 15) was used in order to avoid superpo-

sition of front- and back-layer intensity profiles and to reduce the background. The films were measured with a computer-controlled single-beam microdensitometer LS18, specially designed for this task (12). The collimator slit opening has the dimensions (mm) 0.040×2.0 . Since the cassette radius is 40.16 mm, 0.040 mm along the film translates into 0.0143° or a step-length in 2ϑ of 0.0285° on average. For the exact angle calibration, silicon was added as internal standard ($a = 5.431028 \text{ \AA}$ at 295.7 K (13)). These film data were used for determining the cell parameters of synthetic TiCu_7Se_4 as well as of crookesite.

Another data set was collected without silicon addition for Rietveld refinement, now using a few peaks of the sample itself for calibrating the ϑ -scale with cell parameters obtained from the first data set. This *second* data set is referred to hereafter as GH.

A *third* data set for Rietveld refinement was collected on a STOE STADI/P powder diffractometer using a rotating sample mounted in a symmetric transmission mode. Strictly monochromatic $\text{CuK}\alpha_1$ radiation was obtained from a germanium crystal with a 220-mm radius of curvature. The data were collected with a small position-sensitive detector covering an arc of 4.6° in 2ϑ . It was moved in steps of $0.2^\circ(2\vartheta)$ yielding an average intensity from 23 ($= 4.6^\circ/0.2^\circ$) measurements at each 2ϑ position in order to reduce the influence of errors in the intensity calibration of the detector.

Thus, two independent full-profile Rietveld refinements of the structure were carried out with a local version of the DBW3.2S computer program (14, 15) using the GH and STADI/P data sets. Both refinements were regarded as terminated when all shifts were less than 10% of the corresponding estimated standard deviation of the parameter. The angular dependence of the peak FWHM was expressed as $\text{FWHM}^2 = U \cdot \tan^2 \vartheta + V \cdot \tan \vartheta + W$, where U, V, W are refinable

parameters. The background intensity was approximated by a polynomial expression, the coefficients of which were refined. Further information on the refinements is given in Table II.

Results

The results of the cell parameter refinements are collected in Table I. The values for the synthetic material are consistently smaller than those of a previous determination (1, 6), which had a better resolution. Inadequate weighting of the less resolved data set can hardly have such large effects. Rather, the reason for the discrepancy must be sought in a slight difference in stoichiometry. Considering that previous data yield a difference of 0.04 \AA in the c -axis between the compositions TiCu_7Se_4 and $\text{TiCu}_{6.8}\text{Se}_4$ (translating into 75% and 70% occupancy of one of the eightfold copper sites), the present variance is very small. The difference between the two determinations on crookesite also reflects minute variations in copper content.

As alluded to in the introduction and the experimental section, the single-crystal data of crookesite were not completely satisfactory although rather low R -values were obtained from a refinement in $I4/m$ on the selected data set used: $R_F = 0.085$, $R_{wF} = 0.102$. The standard deviation of "unit-weight normalized data" was 1.974. The refined copper occupancy and all positional parameters are given in Table III.

The two powder data sets were more successfully refined, also in $I4/m$. A trial refinement in space group $I\bar{4}$, suggested for $\text{NH}_4\text{Cu}_7\text{S}_4$, led to divergence. The R -factors (Table II) are considerably lower than that for crookesite. The positional parameters obtained from the powder data are given in Table III.

Figure 1 shows the fit obtained between the calculated and the observed STADI/P

TABLE I
CELL DIMENSIONS (Å UNITS) FROM LEAST-SQUARES REFINEMENTS OF GUINIER-HÄGG DATA WITH SILICON AS INTERNAL STANDARD

Synthetic material				Crookesite		
<i>a</i>	<i>c</i>	<i>M</i> ₂₀	<i>F</i> ₃₀	<i>a</i>	<i>c</i>	Ref.
10.4475(3)	3.9679(2)	94	75(0.009,45)	10.4445(9)	3.9378(4)	This work
10.4524(2)	3.9736(1)	183	175(0.005,35)	10.4456(5)	3.9310(3)	(6)

Note. The accompanying figures within parentheses are the estimated standard deviations. Indexing reliability is given as *M*₂₀ (16) and *F*₃₀ (17).

patterns. Indicated by arrows are some lines of the α-Cu₂Se impurity present (JCPDS 27-1131; (10)), the presence of which marred the data to a minor extent.

The relatively large profile *R*-values for GH refinement (Table II) are caused by the fact that the intensity data from the powder photograph were derived from optical densities above the local background. The true background is not measured. Consequently, the weights cannot be calculated solely from counting statistics from the GH data set. The weighting procedure has recently been discussed in a paper by Eriksson *et al.* (18).

TABLE II
SPECIFIC INFORMATION ABOUT THE RIETVELD REFINEMENTS OF TlCu₇Se₄ IN SPACE GROUP *I4/m* USING GUINIER-HÄGG (GH) AND STADI/P DIFFRACTOMETER DATA

Data set	GH	STADI/P
2θ range	10° ≤ 2θ ≤ 89°	10° ≤ 2θ ≤ 92.5°
2θ step	0.029°	0.01°
Profile function	Modified Lorentzian	Pearson VII
Number of parameters	24	26
Reliability indices ^a		
<i>R</i> _p	0.261	0.064
<i>R</i> _{wp}	0.330	0.082
<i>R</i> _l	0.122	0.084
<i>R</i> _f	0.064	0.064
Durbin-Watson <i>d</i> index:	0.84	0.18

$$^a R_p = \sum |Y_{i,obs} - \frac{1}{c} Y_{i,calc}| / \sum Y_{i,obs}$$

$$R_{wp} = \left\{ \sum w_i |Y_{i,obs} - \frac{1}{c} Y_{i,calc}|^2 / \sum w_i Y_{i,obs}^2 \right\}^{1/2}$$

$$R_l = \sum |f_{obs} - f_{calc}| / \sum f_{obs}, R_f = \sum \left| \frac{|f_{obs}| - |f_{calc}|}{\sum |f_{obs}|} \right|$$

Durbin-Watson *d* statistics (19) which indicate serial correlation were calculated (Table II). As a result, the standard deviations from the Rietveld refinements are underestimated. The errors given in Table III were obtained by multiplying these e.s.d.'s by an ad hoc factor of 2 in order that the positional parameters from the two data sets should not be significantly different.

To account for the ideal stoichiometry, both copper sites cannot be filled to 100%. The refinement on NH₄Cu₇S₄ had shown that the two eightfold sites are filled in the ratio 1 : 0.75. The corresponding result was found for TlCu₇Se₄ with 75% occupancy of the Cu₂ 8*h* site. Although the observed smaller cell volume than previously reported would indicate further nonstoichiometry, the deviation from this ideal value is too small to be discernible from these data. On the other hand, the single-crystal data of crookesite gave conclusive evidence for more substantial copper deficiency although the value found (TlCu_{6.5}Se₄) may be in some doubt considering systematic errors in that data set. Still, the parameter values obtained on stoichiometric material and crookesite, respectively, are very similar.

Discussion and Conclusions

The structure of TlCu₇Se₄ is given in projection along the *c*-axis in Fig. 2. The structure had already been discussed before the refinement, in particular as regards its crys-

TABLE III

CRYSTALLOGRAPHIC DATA OF $\text{TiCu}_{7-x}\text{Se}_4$ AS OBTAINED FROM REFINEMENTS IN SPACE GROUP $I4/m$ ON THE BASIS OF POWDER DATA (FILM AND DIFFRACTOMETER) AND SINGLE-CRYSTAL DATA (ON CROOKSITE).

Site	Atom	GH data		STADI/P		Single crystal (Crook.)		$B_{\text{iso}}(\text{\AA}^2)$
		x	y	x	y	x	y	
2a	Tl	0	0	0	0	0	0	3.9(1)
8h	Cu_1	0.0224(14)	0.3667(10)	0.0197(8)	0.3703(5)	0.0208(7)	0.3680(7)	3.4(2)
8h	Cu_2	0.3213(22)	0.2187(18)	0.3250(10)	0.2210(8)	0.324(1)	0.220(1)	3.6(3)
8h	Se	0.2453(8)	0.4320(8)	0.2441(4)	0.4336(4)	0.2436(5)	0.4309(5)	3.0(1)

Note. All z coordinates are identically zero. The occupancy of the Cu_2 site was refined to 63% for crookesite and to 75% in the powder refinements on the synthetic material. The standard deviations given within parentheses were estimated from the refinements and, in the case of powder data, multiplied by two in order to account for correlation effects as discussed in the text.

tal chemistry in relation to the TiCu_5Se_3 structure (4) although the latter had not been confirmed at the time (2). Further remarks were given in the presentation of isostructural TiCu_7S_4 (7), then still under the assumption that these chalcogenides crystallize in $I\bar{4}$.

One may also recognize elements of the TiCu_2Se_2 structure (20), which contains layers of TiSe_8 cubes, whereas TiCu_7Se_4 only displays columns (Fig. 3). Although not demanded by symmetry, the cubes of different columns are oriented in a manner such that the extrapolation of a cube edge perpendicu-

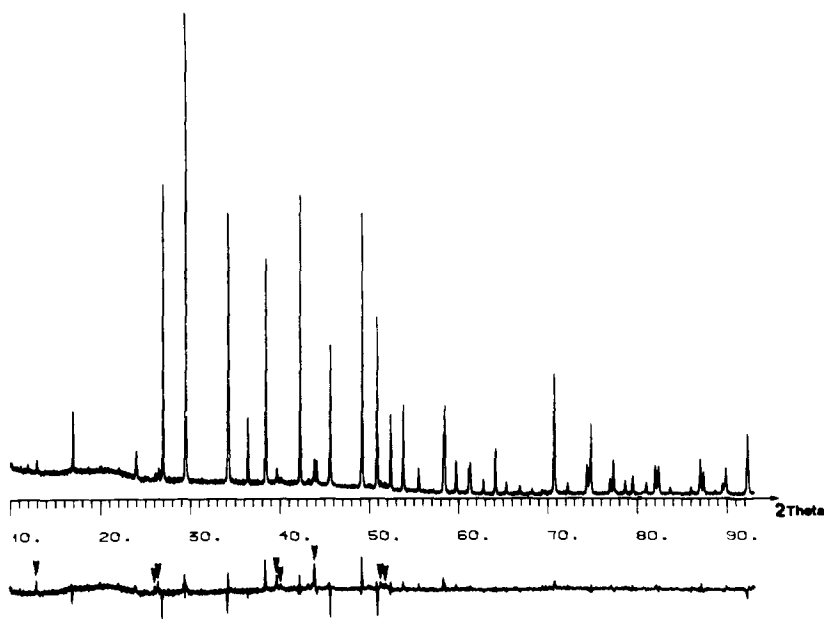


FIG. 1. The final Rietveld profile of TiCu_7Se_4 from the STADI/P data set. The upper curve illustrates the observed data while the lower curve is the difference between observed and calculated data. The arrows at the lower curve indicate diffraction lines of $\alpha\text{-Cu}_2\text{Se}$ present in the sample.

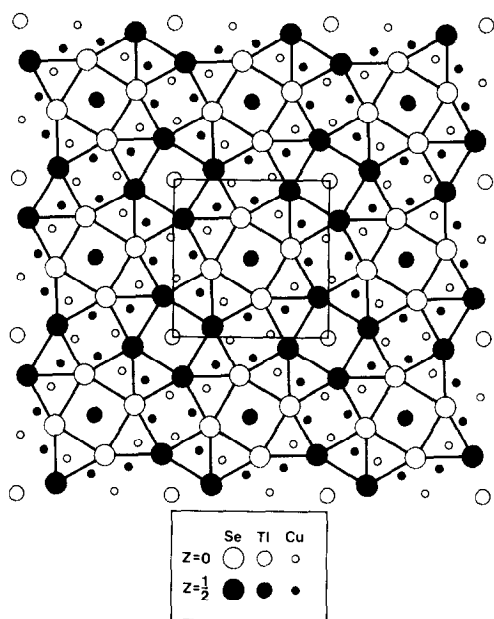


FIG. 2. Projection of the TiCu_7Se_4 structure along $\langle 001 \rangle$. The thin lines indicate the tetragonal unit cell while the thicker lines accentuate the various coordination polyhedra. The copper site with tetrahedral selenium environment is filled only to 3/4.

lar to the column axis very nearly bisects the thallium position within the cube of an adjacent column. This holds exactly for the TiCu_2Se_2 structure where such a line—in fact along $\langle 001 \rangle$ in the structure—also bisects the copper position of the tetrahedral CuSe_4 layers. For the ideal geometry the projection of a selenium tetrahedron (containing Cu_2 in TiCu_7Se_4) is an isosceles triangle. This requirement, adapted to the coordinate system of TiCu_7Se_4 , would enforce a constraint to the parameters of selenium so that $x^2 + y^2 = x$, or in a more convenient form, $x + y^2/x = 1$. The outcome for the right-hand part (\mathcal{R}) of the equation, using parameter values from the best powder refinement given in Table III, is: $\mathcal{R} = 1.014(2)$.

The degree of local higher symmetry may also be tested by calculating the correlation for the *projected* coordinates (to a fixed z) of atoms seemingly lying along such a pseu-

dobisector. Such a line, accentuated in the $\langle 001 \rangle$ projection of Fig. 3 (left), follows Se–Se–Ti–Se–Se. Taking the appropriate coordinates from Table III we arrive at an unweighted correlation coefficient $r = 0.99997$ (compared with $r = 1$ for the constraint occurring in TiCu_2Se_2). The equation of the best fitting line, choosing Ti in the origin, is $y_{\text{proj}} = 1.7513 x_{\text{proj}}$. The orientation corresponds with the $\langle 110 \rangle$ direction in TiCu_5Se_3 and $\langle 001 \rangle$ in TiCu_2Se_2 .

The slope of 1.7513 translates into an angle (γ in Fig. 3) of 29.73° to the b -axis of TiCu_7Se_4 . This structure may be inscribed into that of TiCu_5Se_3 (4), and the angle (α)

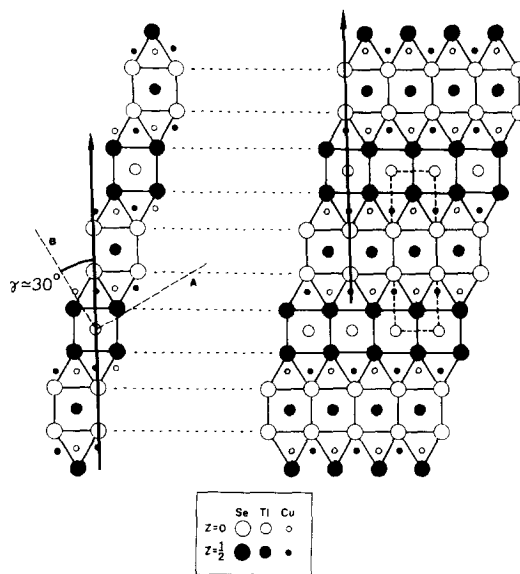


FIG. 3. Left, fragment of the TiCu_7Se_4 structure (cf. Fig. 2) accentuating the coupling between TiSe_8 cube columns and CuSe_4 tetrahedron columns. The thick line running at an angle of about 30° to the b -axis illustrates the local high symmetry and is discussed in the text. The dashed lines sketch the outline of the unit cell as given in Fig. 2. Right, the TiCu_2Se_2 structure in projection along $\langle 010 \rangle$. It may be considered as a condensation product of the fragment given in the left part. The analogue of the line given there runs here along $\langle 001 \rangle$ and is a true bisector owing to symmetry. The unit cell is denoted by dashed lines.

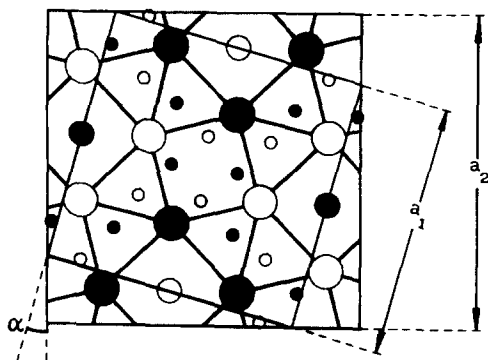


FIG. 4. Crystallochemical relations between the structures of TlCu_7Se_4 and TlCu_5Se_3 in a (001) projection. The TlCu_7Se_4 motif (unit-cell axis a_1) may formally be inscribed into the structure of TlCu_5Se_3 (unit-cell axis a_2). The origin choices here are unconventional, keeping the $\bar{4}$ symmetry at the center in common. From the position of the Tl atom in the two structures, the angle between the two cells is easily derived (see text).

between the respective a -vectors (Fig. 4) may be expressed by the relation $\tan \alpha = 2x/(1 - 2x)$, x now being the coordinate of Tl in TlCu_5Se_3 . The actual x -value of 0.1075 (4) yields $\alpha = 15.32^\circ$. The angle sum, 45.05° , which expresses the orientation of the TlSe_8 cube edges in relation to the b -axis of TlCu_5Se_3 , is very near the ideal value of 45° . Very little structural relaxation is thus needed for adapting the same structural ideas to TlCu_7Se_4 , TlCu_2Se_2 , and TlCu_5Se_3 . This also lies implicit in the relative values of the a -axes (a_1 and a_2 denote the values for TlCu_7Se_4 and TlCu_5Se_3 , respectively, as illustrated in Fig. 4) where, on the same basis, one would expect $(a_1/a_2)^2 = 4x(2x - 1) + 1$; the experimental x -parameter yields an expected axis ratio of 0.814 compared with the actual value of 0.810 (1).

It is obvious that simple geometrical arguments are valid to a large extent because of the crystal-chemical rigidity, previously demonstrated in structural relations between $\text{TlCu}_7\text{S}_4/\text{TlCu}_3\text{S}_2$ (7) and $\text{Tl}_5\text{Cu}_{14}\text{Se}_{10}/\text{TlCu}_3\text{Se}_2$ (2, 3, 5). Extensive intergrowth is then likely in cases where the actual compo-

sition deviates from the ideal stoichiometry. In Fig. 3, the structural relations between TlCu_7Se_4 and TlCu_2Se_2 are illustrated. In Fig. 5 we present a strongly coherent crystal fault that accommodates copper deficiency by applying these ideas. The reason for the difficulty in obtaining good single crystal material of crookesite might be sought in such a mechanism.

In the light of the crystal-chemical rigidity the interatomic distances, displayed in Table IV, show values within expectation. The CN8 of Tl vs Se creates Tl-Se distances compatible with those found in TlCu_5Se_3 (4) and $\text{Tl}_5\text{Cu}_{14}\text{Se}_{10}$ (5), being somewhat longer than those obtained for CN7 in TlCu_3Se_2 (3) and $\text{Tl}_5\text{Cu}_{14}\text{Se}_{10}$ (5). A corresponding tendency is found for the CN3 compared to the CN4 Cu-Se distances. The shortest Cu-Cu distance is 2.56 Å.

It is interesting to note that the copper deficiency (such as in crookesite) may be

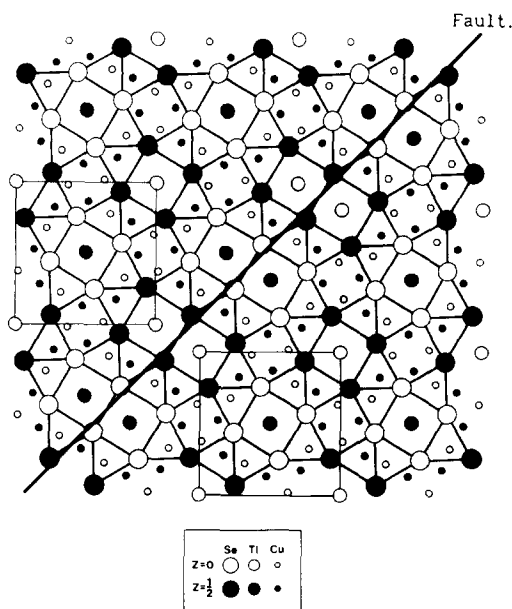


FIG. 5. Tentative coherent stacking fault in copper-deficient TlCu_7Se_4 obtained by applying the crystal chemical ideas developed in Fig. 3.

TABLE IV
INTERATOMIC DISTANCES (AND STANDARD
DEVIATIONS) IN Å UNITS OF TiCu_7Se_4 AS OBTAINED
FROM THE STADI/P DATA SET

Cu_1 —Se	2.436(4)	Cu_2 —Se	2.377(5)
Cu_1 —2Se	2.485(2)	Cu_2 —Se	2.534(6)
Cu_1 — Cu_2	2.559(6)	Cu_2 — Cu_1	2.559(6)
Cu_1 —2 Cu_2	2.735(4)	Cu_2 —2 Cu_2	2.600(7)
Cu_1 — Cu_1	2.741(5)	Cu_2 —2Se	2.658(3)
Cu_1 —4 Cu_1	2.774(3)	Cu_2 —2 Cu_1	2.735(4)
Cu_1 —Se	3.434(4)	Cu_2 — Cu_1	3.551(7)
Cu_1 — Cu_2	3.551(7)	Cu_2 — Cu_1	3.815(6)
Cu_1 — Cu_2	3.815(6)		
Cu_1 —Ti	3.874(3)		
		Tl—8Se	3.401(1)
Se—2Se	3.906(3)	Tl—4 Cu_1	3.874(3)

Note. Distances up to 3.95 Å are given. The coordination of metal atoms about selenium can be calculated from the other data in the table.

enforced by chemical means (1, 2) and that the products, as well as the mineral, are metallic conductors. Copper extraction probably creates valence-band holes, as indicated by a positive slope of the Seebeck coefficient vs temperature. This slope decreases on enhanced copper deficiency, a sign that the Fermi energy increases (1). Further research is intended in this area to clarify the relation between structure and electrical transport properties.

In conclusion, we have confirmed that TiCu_7Se_4 (synthetic crookesite) crystallizes in $I4/m$. We believe that natural crookesite, despite difficulties with the single-crystal structure refinement, is also truly tetragonal and not subject to any change in symmetry on grounds of the deviation in copper content. Renewed research on $\text{NH}_4\text{Cu}_7\text{S}_4$ and TiCu_7S_4 should show that they are truly isostructural.

Acknowledgments

The skillful technical assistance by Mr. Lars Göthe is much appreciated. The new sample of crookesite was put to our disposal through Dr. P. Nysten, Institute of Geology, University of Uppsala. This work received financial support from the Swedish Natural Science Research Council (NFR).

References

1. R. BERGER, *J. Solid State Chem.* **70**, 65 (1987).
2. R. BERGER, *Chem. Scr.* **28**, 41 (1988).
3. R. BERGER AND L. ERIKSSON, *J. Less-Common Met.* **161**, 101 (1990).
4. R. BERGER, L. ERIKSSON, AND A. MEERSCHAUT, *J. Solid State Chem.* **87**, 283 (1990).
5. R. BERGER AND A. MEERSCHAUT, *Eur. J. Solid State Inorg. Chem.* **25**, 279 (1988).
6. R. A. BERGER, *Z. Kristallogr.* **181**, 241 (1987).
7. R. A. BERGER AND R. J. SOBOTT, *Monatsh. Chem.* **118**, 967 (1987).
8. G. GATTOW, *Acta Crystallogr.* **10**, 549 (1957).
9. Z. JOHAN, *C.R. Acad. Sci. Paris, Ser. II*, **18**, 1121 (1987).
10. R. M. MURRAY AND R. HEYDING, *Canad. J. Chem.* **53**, 878 (1975).
11. J. W. EARLEY, *Amer. Mineral.* **35**, 337 (1950).
12. K.-E. JOHANSSON, T. PALM, AND P.-E. WERNER, *J. Phys.* **E13**, 1289 (1980).
13. M. DEUTSCH AND M. HART, *Phys. Rev. B* **26**, 5558 (1982).
14. D. B. WILES AND R. A. YOUNG, *J. Appl. Crystallogr.* **14**, 149 (1981).
15. D. B. WILES, A. SAKTHIVEL, AND R. A. YOUNG, *Program DBW 3.2S* (1987).
16. P. M. DE WOLFF, *J. Appl. Crystallogr.* **1**, 108 (1968).
17. G. S. SMITH AND R. L. SNYDER, *J. Appl. Crystallogr.* **12**, 60 (1979).
18. L. ERIKSSON, D. LOUËR AND P.-E. WERNER, *J. Solid State Chem.* **81**, 9 (1989).
19. R. J. HILL AND H. D. FLACK, *J. Appl. Crystallogr.* **20**, 356 (1987).
20. R. BERGER AND C. F. VAN BRUGGEN, *J. Less-Common Met.* **99**, 113 (1984).
21. R. BAIER AND R. HOPPE, *Z. Anorg. Allg. Chem.* **568**, 136 (1989).
22. R. HOPPE, E. SEIPP AND R. BAIER, *J. Solid State Chem.* **72**, 52 (1988).